Am J Transl Res 2026;18(7):6069-6082
www.ajtr.org /ISSN:1943-8141/AJTR0173387

Original Article

LncRNA OTUD6B-AS1 overexpression induces parthanatos in esophageal adenocarcinoma cells by binding to miR-145-5p and promoting AIF expression

Qingfeng Zheng[1], Qiuli Wu[1], Yuling Lin[2], Xiangbo Chen[1]

[1]Gastrointestinal Endoscopy Room, Quanzhou First Hospital, Quanzhou 362000, Fujian, China; [2]Clinical Laboratory, Quanzhou First Hospital, Quanzhou 362000, Fujian, China

Received April 17, 2026; Accepted June 17, 2026; Epub July 15, 2026; Published July 30, 2026

Abstract: Objectives: To investigate the functional role of OTU deubiquitinase 6B-antisense transcript 1 (OTUD6B-AS1) and its potential association with parthanatos - a poly (ADP-ribose) polymerase 1 (PARP-1)/apoptosis-inducing factor (AIF)-mediated regulated cell death pathway - in esophageal adenocarcinoma (EAC), which remains poorly understood. Methods: The expression patterns of OTUD6B-AS1, miR-145-5p, and its downstream target AIF protein were investigated in EAC cell lines. Gain- and loss-of-function assays were performed *in vitro* and *in vivo* to evaluate biological effects. The competing endogenous RNA (ceRNA) regulatory mechanism was verified using dual-luciferase reporter assays and RNA immunoprecipitation (RIP) assays. Activation of parthanatos was assessed by detecting AIF nuclear translocation and DNA damage levels. Result: OTUD6B-AS1 was reduced significantly, and predominantly localized in the cytoplasm of EAC cells. OTUD6B-AS1 overexpression significantly inhibited EAC cell proliferation, migration, and invasion, and induced cellular apoptosis. Mechanistically, OTUD6B-AS1 functioned as a ceRNA, competitively binging to miR-145-5p and thereby relieving its translational suppression of AIF. This biological pathway promoted parthanatos activation, as evidenced by PARP-1 upregulation, extensive DNA damage (with γ-H2AX deposition), and nuclear translocation of AIF. OTUD6B-AS1-induced antitumor activities were abolished by miR-145-5p overexpression or AIF knockdown. Consistently, OTUD6B-AS1 overexpression substantially suppressed xenograft tumor growth *in vivo*. Conclusion: OTUD6B-AS1 suppresses EAC progression by sponging miR-145-5p and upregulating AIF to induce parthanatos activation. Targeting this ceRNA regulatory axis may be a therapeutic strategy for EAC.

Keywords: Esophageal adenocarcinoma, OTUD6B-AS1, parthanatos, miR-145-5p

Introduction

Esophageal adenocarcinoma (EAC) at an advanced stage generally lacks actionable targets for effective targeted therapy. Over the past 40 years, its incidence has been steadily increasing. The five-year survival rate of EAC is approximately 18.0%, and a substantial proportion of patients present with unresectable locally advanced disease, inoperable tumors, or distant metastasis [1, 2]. EAC commonly arises from Barrett's esophagus (BE), a condition characterized by intestinal metaplasia in the distal esophagus below the gastroesophageal junction, which develops under prolonged exposure to bile reflux and chronic inflammatory stimulation. Currently, treatment strategy for locally advanced EAC involves neoadjuvant chemoradiotherapy, alone or in combination, followed by surgical resection. However, fewer than 30% of patients achieve a pathologic complete response after neoadjuvant chemotherapy [3, 4]. Therefore, it is essential to further elucidate the molecular mechanisms underlying EAC progression and identify novel therapeutic targets to improve patient prognosis.

Parthanatos is a distinct form of programmed cell death mediated by overactivation of poly (ADP-ribose) polymerase 1 (PARP-1) [5, 6]. Unlike conventional apoptosis, parthanatos is characterized by excessive PARP-1 activation, extensive DNA damage, nuclear translocation of apoptosis-inducing factor (AIF), resulting in

https://doi.org/10.62347/MLEF4848

caspase-independent cell death. As a form non-apoptotic regulated cell death, parthanatos has attracted increasing attention in oncology, particularly for its potential to overcome apoptosis resistance in cancer therapy.

AIF is a mitochondrial flavoprotein that acts as an essential regulator of parthanatos. Evidence suggests that promoting AIF nuclear translocation to induce parthanatos in cancer cells may inhibit tumor proliferation and facilitate immunosurveillance evasion [7]. In colorectal cancer, pharmacologic or genetic inhibition of AKT has been shown to activate p53-dependent Sirtuin 6 (SIRT6) and PARP-1 signaling, leading to AIF release and nuclear translocation, thereby triggering parthanatos and promoting colorectal cancer cell death [8]. Previous studies have also demonstrated that inhibiting PARP-1 expression can suppress the proliferation and metastatic potential of EAC cells (e.g., OE33 and JHesoAD1) [9]. Nevertheless, to date, whether PARP-1-AIF-mediated parthanatos contributes to the progression of EAC remains underexplored.

MicroRNA (miRNAs) are single-stranded, small non-coding RNAs with an average length of approximately 19-24 nucleotides and high evolutionary conservation and stability. They regulate gene expression by binding to complementary sequences in target mRNAs, thereby promoting mRNA degradation or inhibiting protein translation [10, 11]. Previous studies have shown that miR-421 and miR-550a-3p are significantly upregulated in neoplastic tissues, and their simultaneous downregulation effectively inhibit the proliferation, migration, and invasion of OE33 cells, suggesting a favorable prognosis [12]. Additionally, miR-145-5p is elevated in EAC and has been implicated in tumor immune evasion [13]. Recent evidence further indicates that miR-145-5p inhibits apoptosis by targeting AIF [14]. These findings suggest that miR-145-5p may contribute to tumor cell death by modulation of the parthanatos pathway and may represent a key regulatory factor in EAC progression.

Long non-coding RNAs (lncRNAs) are a class of non-coding transcripts longer than 200 nucleotides that regulate gene expression at multiple levels. lncRNAs can competitively interact with microRNAs to regulate the expression of downstream target genes through the competitive-endogenous-RNA (ceRNA)-regulated network, thereby participating in tumor proliferation, invasion, and treatment resistance [15]. Also significantly impacts the growth of EAC-related lncRNAs. For example, lncRNA-MIR22HG is overexpressed in malignant EAC tissues; its knockdown inhibits activation of the STAT3/c-Myc/p-FAK signaling pathway and induces apoptosis in EAC cells [16]. LncRNA OTU Deubiquitinase 6B-Antisense Transcript 1 (OTUD6B-AS1) has recently emerged as a context-specific regulator of oncogenic progression. In non-small cell lung cancer, OTUD6B-AS1 levels is downregulated and functions as a tumor suppressor by inhibiting epithelial-to-mesenchymal transition (EMT) and promoting apoptosis through modulation of the Wnt/β-catenin signaling pathway [17]. Similarly, OTUD6B-AS1 suppresses proliferation and migration in thyroid cancer [18]. Nevertheless, the biologic function of OTUD6B-AS1 in EAC remains undefined. We hypothesized that OTUD6B-AS1 may act as a molecular sponge for miR-145-5p, thereby restoring AIF expression, activating PARP-dependent parthanatos, and ultimately inducing cell death in EAC.

In this study, we investigated the OTUD6B-AS1/miR-145-5p/AIF regulatory axis and its role in modulating parthanatos in EAC using both *in vitro* and *in vivo* experimental models. Our findings may provide a mechanistic theoretical basis for developing targeted therapeutic strategies for advanced EAC, thereby improving clinical outcome.

Materials and methods

Cell culture and cell transfection

The human normal esophageal epithelial cell line Het-1A and EAC cell strain, including OE33, FLO-1, SK-GT-4, were obtained from American Type Culture Collection (ATCC; Manassas, VA, USA). Het-1A cells were cultured in bronchial epithelial cell growth medium (BEGM, Lonza), while EAC cell lines were maintained in RPMI-1640 medium (Gibco, Grand Island, New York, USA). All media contained 10% fetal bovine serum (FBS; Gibco) and 1% penicillin-streptomycin solution. Cells were incubated at 37°C in a humidified atmosphere containing 5% CO_2.

Lentiviral constructs encoding the full-length OTUD6B-AS1 (OE-OTUD6B-AS1) and corres-

ponding negative control vector (OE-NC) were generated by GeneChem (Shanghai, China). OE33 and FLO-1 cells at approximately 50%-60% confluence were transfected with the above lentiviruses using Lipofectamine 3000 (Invitrogen; Carlsbad, CA, USA). Polybrene (8 μg/mL; Sigma-Aldrich, TR-1003) and lentiviral particles at a multiplicity of infection (MOI) of 10 were added to enhance transduction efficiency. After 48 h of culture, stable transfectants were selected using puromycin (2 μg/mL) for about 7 days. Overexpression efficiency of OTUD6B-AS1 was verified by quantitative real-time PCR (qRT-PCR).

Subcellular fractionation assay

To characterize the cellular localization of OTUD6B-AS1, the PARIS™ kit (Invitrogen, Carlsbad, CA, USA) was used to isolate nuclear and cytoplasmic fractions as per manufacturer's instructions. RNA extracted from each fraction was subsequently analyzed by qRT-PCR. U6 small nuclear RNA (snRNA) and GAPDH were used as internal controls for nuclear and cytoplasmic fractions, respectively.

RNA fluorescence in-situ hybridization (RNA-FISH)

Cells grown on glass coverslips were fixed with 4% paraformaldehyde, permeabilized using 0.5% Triton X-100, and hybridized overnight at room temperature in the dark with a customized OTUD6B-AS1 probe (RiboBio, Guangzhou, China). After stringent washing to remove unbound probes, nuclei were counterstained using DAPI (Sigma-Aldrich, St. Louis, MO). Fluorescence signals were visualized using a confocal laser scanning microscope.

Quantitative real-time PCR (qRT-PCR)

Total RNA from cultured cells was extracted using TRIzol reagent (Invitrogen, Carlsbad, CA, USA) according to the manufacturer's instructions. For lncRNA analysis, cDNA was synthesized using PrimeScript RT-PCR reagents kit (Takara Bio Inc. China). For miRNA detection, reverse transcription was performed using the Mir-X™ miRNA First-Strand Synthesis Kit (Takara). qRT-PCR was conducted using the ABI 7500 Fast system (Applied Biosystems) with SYBR Premix Ex Taq (Takara). Relative gene expressions levels were calculated using $2^{-\Delta\Delta Ct}$. GAPDH or U6 served as the internal reference for OTUD6B-AS1 and miR-145-5p, respectively.

Western blot analysis

Total cellular proteins were extracted using RIPA lysis buffer. Protein concentrations were quantified using a BCA Protein Assay Kit (Pierce). Equivalent amounts of protein were separated by SDS-PAGE and electro-transferred onto PVDF membrane (Millipore, Billerica, MA, USA). After nonfat milk (5%) block, the membranes were incubated overnight at 4°C with primary antibodies against AIF (Abcam, ab32516, 1:1000), γ-H2AX (Abcam, ab26350, 1:2000), PARP-1 (Abcam, ab191217, 1:1000), and GAPDH (Abcam, ab8245, 1:2500). After washing, membranes were incubated with HRP-labeled secondary antibodies (Abcam, ab205718, 1:5000). Protein bands were visualized using an ECL detection kit (Bio-Rad).

Cell counting kit-8 (CCK-8) assay

Cell proliferation was assessed using a Cell Counting Kit-8 (CCK-8; Sigma-Aldrich, St. Louis, MO, USA). Transfected cells were seeded into 96-well microplates at a density of 2×10^3 cells/well. After incubation for 72 h, 10 μL of CCK-8 solution was added into each well and then incubated at 37°C for another two hours. The absorbance was measured at 450 nm using a specific-wavelength microplate reader (BioTek, USA), and cell viability was expressed as optical density (OD) values.

Wound healing assay

Cell migratory ability was assessed using a wound healing assay. Cells were seeded into six-well plates and cultured until reaching near-confluent monolayers. A straight scratch was created using a sterile 200-μL pipette tip to generate a cell-free gap. Detached cells were removed by washing with PBS, and the remaining cells were cultured in serum-free medium. Images of wound closure were captured at 0 h and 48 h using an inverted phase-contrast microscope (Olympus, Japan). Cell migration ability was quantified by measuring the reduction in wound area over time.

Transwell invasion assay

Cell invasion ability was assessed using Transwell chambers with 8 μm pore size membranes (Corning, New York) coated with Matrigel (BD Biosciences). Approximately 5 × 10^4 cells suspended in 200 μL of serum-free medium were added into the upper chamber. The lower compartment was filled with 600 μL of complete medium containing 10% FBS as a chemoattractant. After incubation for 48 h at 37°C, non-invading cells were gently removed. Cells successfully invaded were fixed with 4% paraformaldehyde and stained with crystal violet (Sigma-Aldrich, St. Louis, MO). Invaded cells were visualized and counted in five randomly selected microscopic fields per membrane.

Flow cytometry

Cell death was measured using an Annexin V-FITC/PI apoptosis detection kit (BD Biosciences) according to the manufacturer's instructions. Both attached and detached cells were collected, washed twice with cold PBS solution, then resuspended in binding buffer. Cells were then stained with annexin V-FITC and PI for 15 minutes at room temperature in the dark. Samples were analyzed immediately using a BD FACSCanto II flow cytometer (BD Biosciences). The total cell death rate was calculated as the sum of early apoptosis, late apoptosis, and necrotic cell populations.

Immunofluorescence (IF) staining

To evaluate the subcellular relocation of AIF, cells grown on glass coverslips were fixed using 4% paraformaldehyde for 20 min and then permeabilized with 0.3% Triton X-100. After blocking with 5% bovine serum albumin for 1 h at room temperature, cells were then incubated over night at 4°C with an anti-AIF primary antibody (Abcam, ab32516, 1:200). After washing, cells were incubated with fluorophore-conjugated secondary antibodies (Alexa Fluor 488; Abcam, ab150077, 1:500) for 1 hour at room temperature. Nuclei were counterstained with DAPI, and fluorescence signals were visualized using a confocal microscope (Leica, Wetzlar, Germany).

Dual-luciferase reporter assay

Putative miR-145-5p binding sites within OTUD6B-AS1 and their corresponding mutant sequences were amplified and cloned into pmirGLO dual-luciferase reporter vector (Promega, Madison, WI, USA) to create WT-OTUD6B-AS1 and Mut-OTUD6B-AS1 constructs respectively. Cells were seeded in 24-well plates and co-transfected with 100 ng reporter plasmid and either 50 nM miR-145-5p mimics or negative control mimic using Lipofectamine 3000 (Invitrogen). After 48 hours of transfection, luciferase activity was detected using a dual-luciferase reporter assay kit (Promega Corporation, USA). Renilla luciferase activity was used for internal control.

RNA immunoprecipitation (RIP) assay

RNA immunoprecipitation (RIP) assays were performed using the Magna RIP™ RNA-Binding Protein Immunoprecipitation Kit (Millipore) according to the manufacturer's instructions. Specifically, magnetic beads were incubated overnight at 4°C with either anti-Ago2 antibody (Abcam) or isotype-matched normal mouse IgG as a negative control. After removing non-specifically bound components by washing, RNA-protein complexes were immunoprecipitated. The co-precipitated RNA was extracted and purified, and the enrichment of OTUD6B-AS1 and miR-145-5p was quantified using qRT-PCR.

In vivo xenograft tumor model

All animal experiments were approved by the Institutional Animal Care and Use Committee of Quanzhou First Hospital. Males of BALB/c nude mice (4-5 weeks old) were obtained from a specific pathogen-free facility. Xenograft tumorigenicity test was conducted as follows: OE33 cells stably transfected with OE-NC or OE-OTUD6B-AS1 were harvested and resuspended in ice-cold PBS. The cell suspension was mixed with an equal volume of Matrigel (Corning, NY, USA) to a final concentration of 1 × 10^6 cells/mL and then subcutaneously injected into the right flank of each mouse (n = 5 per group). Tumor growth was monitored weekly, and tumor volume was calculated using a standard formula: V = 0.5 × length × $width^2$. After a 28-day observation period, mice were humanely euthanized by cervical dislocation, and xenografts were excised, photographed, and weighed.

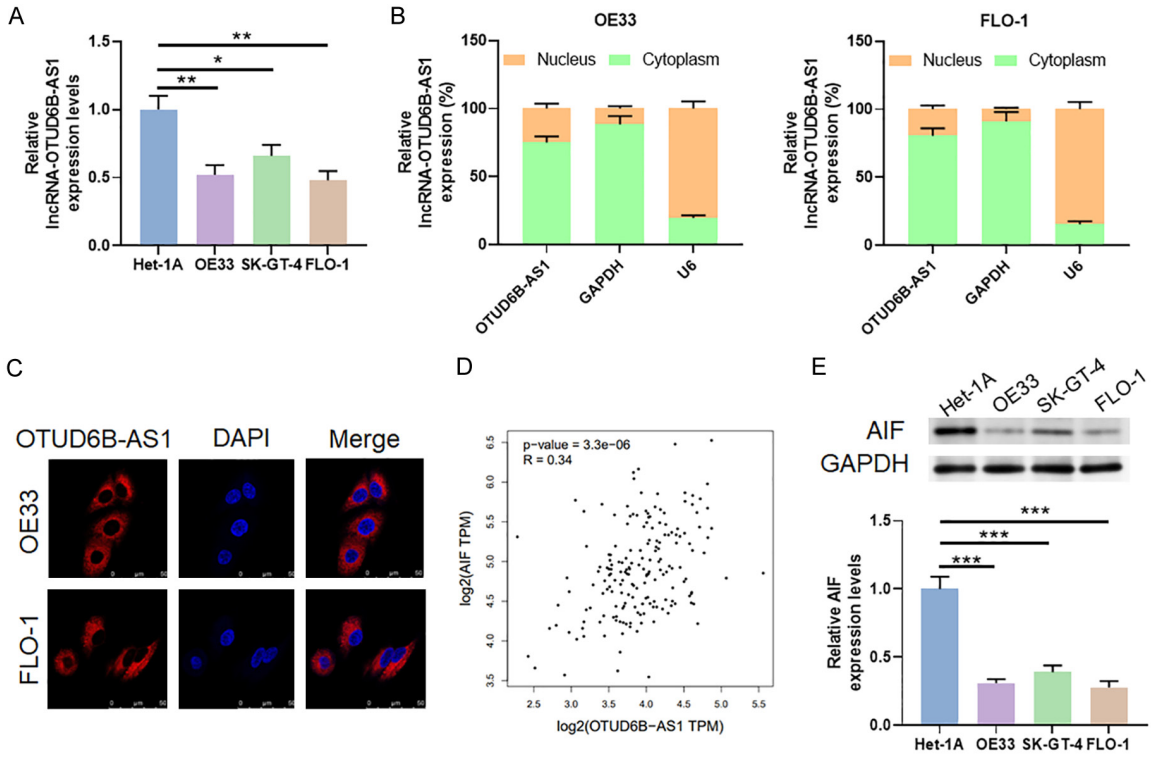

Figure 1. Expression and subcellular localization of OTUD6B-AS1 in esophageal adenocarcinoma (EAC) cell lines. A. qRT-PCR analysis of OTUD6B-AS1 expression in Het-1A and EAC cell lines (OE33, FLO-1, SK-GT-4). B. Sub-cellular fractionation assay showing the distribution of OTUD6B-AS1 in the nuclear and cytoplasmic compartments of OE33 and FLO-1 cells. C. Representative RNA fluorescence in-situ hybridization (RNA-FISH) images demonstrating cytoplasmic localization of OTUD6B-AS1 (red). Cell nuclei were counterstained with 4',6-diamidino-2-phenylindole (DAPI). Scale Bar = 50 μm. D. Correlation analysis between OTUD6B-AS1 and apoptosis-inducing factor (AIF) expressions using data from the GEPIA Database. E. Western blot analysis of AIF protein expression in Het-1A and EAC cell lines. **P*<0.05, ***P*<0.01, ****P*<0.001.

Statistical analysis

All data were expressed as mean ± standard deviation (SD) from at least three independent experiments. Statistical analyses were performed using GraphPad Prism Version 8.0 (San Diego, California, USA). Comparisons between two groups were performed using unpaired Student's t-tests, while comparisons among multiple groups were performed using one-way ANOVA followed by Tukey's post hoc test. A *P* value <0.05 was considered significant.

Results

Downregulation of OTUD6B-AS1 and its association with AIF in EAC cells

We first characterized the endogenous expression pattern of OTUD6B-AS1 in EAC using qRT-PCR. The results demonstrated that OTUD6B-AS1 expression was significantly decreased across multiple EAC cell lines compared to Het-1A cells (**Figure 1A**).

We further examined the intracellular distribution of OTUD6B-AS1 in OE33 and FLO-1 cells. Nuclear-cytoplasmic fractionation analysis revealed that OTUD6B-AS1 was primarily localized in the cytoplasmic fraction (**Figure 1B**). RNA-FISH also confirmed strong cytoplasmic fluorescence of OTUD6B-AS1 in EAC cells (**Figure 1C**).

To clarify the potential downstream associations, bioinformatic analysis was performed with GEPIA database. A significant positive correlation was observed between OTUD6B-AS1 and AIF expressions (**Figure 1D**). Furthermore, western blotting analysis verified a corresponding decrease in AIF protein levels in EAC cell lines compared with Het-1A cells (**Figure 1E**). Collectively, these findings indicated that both OTUD6B-AS1 and AIF are downregulated in EAC

cells, suggesting a regulatory relationship between them.

Ectopic expression of OTUD6B-AS1 suppressed malignant phenotypes of EAC cells

To investigate the functional role of OTUD6B-AS1 in EAC, OE33 and FLO-1 cells were transfected with lentiviral vectors to overexpress OTUD6B-AS1. qRT-PCR confirmed successful overexpression in the OE-OTUD6B-AS1 group compared to the OE-NC group (**Figure 2A**).

CCK-8 assay showed that OTUD6B-AS1 overexpression significantly reduced cell proliferation over a 72-h period (**Figure 2B**). Furthermore, flow cytometry analysis showed that OTUD6B-AS1 overexpression increased the proportion of apoptotic cells (**Figure 2C**). In addition, wound healing assays revealed that OTUD6B-AS1 overexpression markedly reduced the migratory capacity of EAC cells, evidenced by a decreased wound closure rate compared to the control group (**Figure 2D**). Consistently, Transwell invasion assay showed that the number of invading cells was significantly decreased after OTUD6B-AS1 overexpression (**Figure 2E**).

OTUD6B-AS1 promoted parthanatos-associated cell death by enhancing DNA damage and AIF nuclear translocation

Given the pronounced cytotoxic effects induced by OTUD6B-AS1 overexpression, we further explored the underlying molecular mechanisms driving cell death in EAC cells. Based on bioinformatic findings, a potential regulatory association among OTUD6B-AS1, AIF, and the parthanatos pathway was suggested. Western blot analysis showed that, compared to the control group, OTUD6B-AS1 overexpression significantly increased the protein expression of PARP-1 and AIF in OE33 and FLO-1 cells (**Figure 3A-C**). In addition, an obvious increase in γ-H2AX accumulation was observed, indicating enhanced DNA damage (**Figure 3D**).

To further assess subcellular dynamics of AIF, confocal immunofluorescence analysis was performed. AIF was mainly localized at the cytoplasm in control OE33 and FLO-1 cells; however, OTUD6B-AS1 overexpression induced a significant nuclear translocation of AIF (**Figure 3E**). This nuclear translocation of AIF, together with PARP-1 activation and DNA damage accumulation, is consistent with activation of parthanatos-related cell death signaling.

OTUD6B-AS1 functions as a ceRNA to sponge miR-145-5p and relieve AIF repression

Considering the cytoplasmic localization of OTUD6B-AS1, we hypothesized that it may regulate gene expression through a ceRNA mechanism. Bioinformatics analysis using the starBase database (http://starbase.sysu.edu.cn/) identified potential binding sites between OTUD6B-AS1 and miR-145-5p, as well as between miR-145-5p and the 3'-UTR of AIF (**Figure 4A**).

qRT-PCR results showed that miR-145-5p expression was significantly higher in EAC cells compared to Het-1A cells (**Figure 4B**). Dual-luciferase reporter gene assay demonstrated that miR-145-5p mimics significantly reduced the activity of the WT-type OTUD6B-AS1 reporter, whereas mutation the binding site abolished this effect (**Figure 4C**). In addition, RIP assays using Ago2 antibodies confirmed that OTUD6B-AS1 and miR-145-5p were simultaneously enriched in the RNA-induced silencing complex (**Figure 4D**). Mechanistically, overexpressing OTUD6B-AS1 significantly reduced the level of endogenous miR-145-5p (**Figure 4E**), supporting its role as a functional miRNA sponge.

To determine whether miR-145-5p regulate AIF, dual-luciferase experiments further confirmed that miR-145-5p directly binds to the 3'-UTR of AIF (**Figure 4F**). Consistently, western blot analysis showed that transfection of miR-145-5p mimics reduced AIF protein expression in EAC cells (**Figure 4G**).

OTUD6B-AS1/miR-145-5p/AIF pathway regulated proliferation and apoptosis of EAC cells

To clarify whether the oncogenic effects of OTUD6B-AS1 are mediated through the miR-145-5p/AIF axis, gain-and-loss-of-function rescue assays were performed. Western blot analysis showed that the elevated increased expression of AIF and γ-H2AX induced by OTUD6B-AS1 overexpression was significantly attenuated by co-transfection with miR-145-5p mimics or si-AIF (**Figure 5A-C**). This molecule-restoration offered the impetus for further phenotypic evaluation.

Functionally, CCK-8 assays showed that the inhibitory effect of OTUD6B-AS1 on cell proliferation was notably rescued after miR-145-5p overexpression or AIF knockdown in OE33 and FLO-1 cells (**Figure 5D**). Similarly, the suppressive of OE-OTUD6B-AS1 on cell migration and

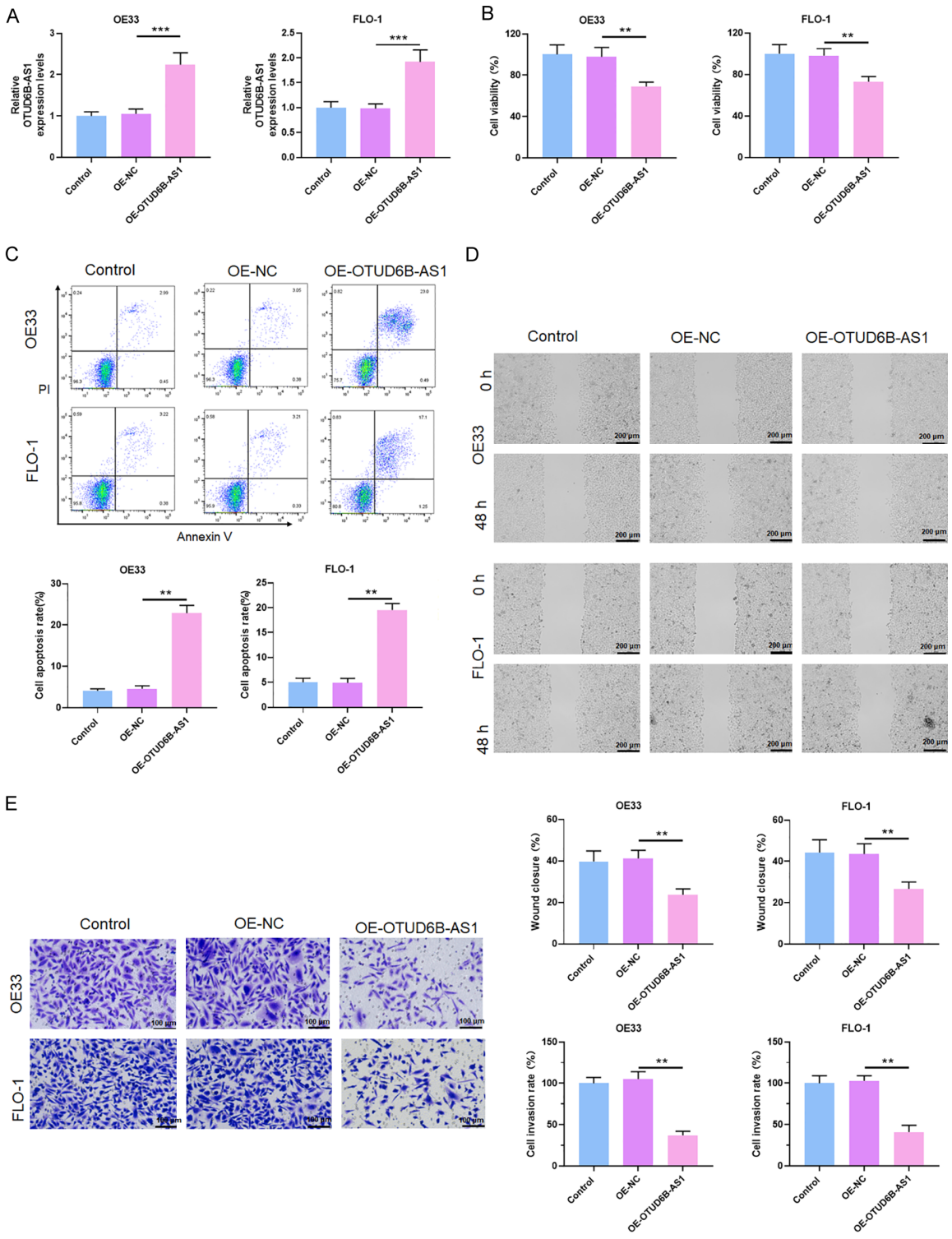

Figure 2. Effect of OTUD6B-AS1 overexpression on the malignant phenotype of EAC cells. A. qRT-PCR validation of OTUD6B-AS1 overexpression in EAC cells. B. Cell proliferation curves measured by the CCK-8 assay over a 72-hour period. C. Flow cytometric analysis of total cell death in OTUD6B-AS1-overexpressing EAC cells. D. Wound healing assay evaluating cell migration potential at 0 hours and 48 hours. Scale Bar = 200 μm. E. Transwell invasion assay evaluating the invasive ability of OTUD6B-AS1 overexpressing EAC cells. Scale Bar = 100 μm. ***P*<0.01, ****P*<0.001.

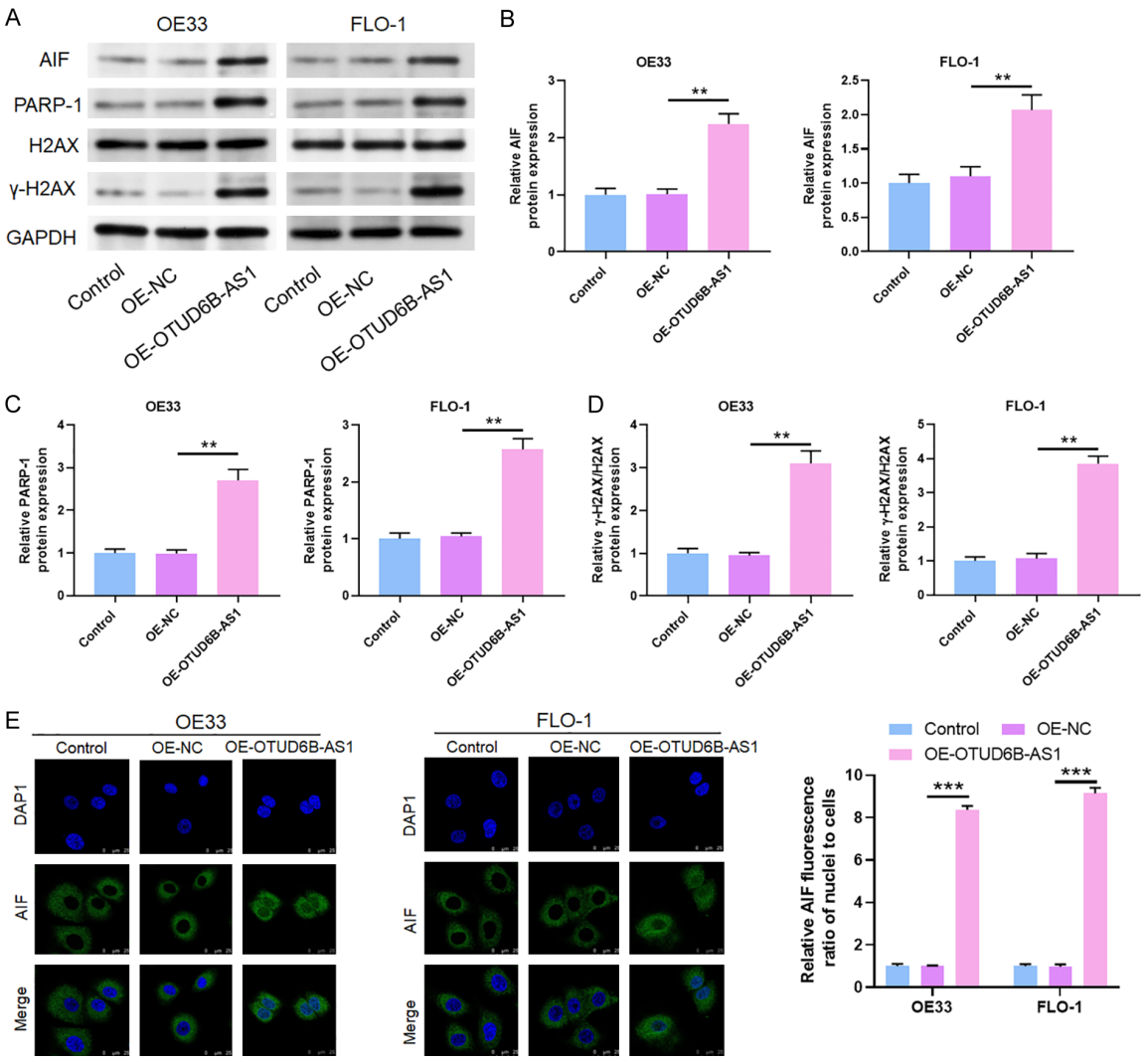

Figure 3. Effect of OTUD6B-AS1 on parthanatos-associated signaling, characterized by AIF nuclear translocation and DNA damage. A. Western blot analysis of AIF and PARP-1, and γ-H2AX expression in OE33 and FLO-1 cells after overexpressing OTUD6B-AS1. B-D. Quantitative densitometric analysis of AIF, PARP-1, and γ-H2AX protein levels normalized to GAPDH. E. Representative immunofluorescence images showing nuclear translocation of AIF (green) in OE-OTUD6B-AS1-overexpressing cells. Nuclei were stained with 4',6-diamidino-2-phenylindole (DAPI; blue). Scale Bar = 25 μm. ***P*<0.01, ****P*<0.001.

invasion were significantly reversed after miR-145-5p overexpression or AIF silencing, as evidenced by accelerated wound closure and increased numbers of invaded cells (**Figure 5E-H**).

OTUD6B-AS1 suppressed EAC tumorigenicity in vivo by the miR-145-5p/AIF parthanatos axis

To validate the *in vitro* findings, a subcutaneous xenograft model in nude mice was established. OTUD6B-AS1 overexpression significantly inhibited tumor growth compared with the control group, as evidenced by reduced tumor volume over time (**Figure 6A**, **6B**). Consistently, the mean tumor weight was significantly lower in the OE-OTUD6B-AS1 group (**Figure 6C**). H&E-staining and TUNEL-staining data showed increased apoptotic cell death in tumors from the OE-OTUD6B-AS1 group (**Figure 6D** and **6E**).

qRT-PCR confirmed sustained upregulation of OTUD6B-AS1 in xenograft tissues, along with a significant decrease in endogenous miR-145-5p levels (**Figure 6F** and **6G**). Furthermore, western blot analysis of tumor tissues revealed significantly increased AIF protein expression

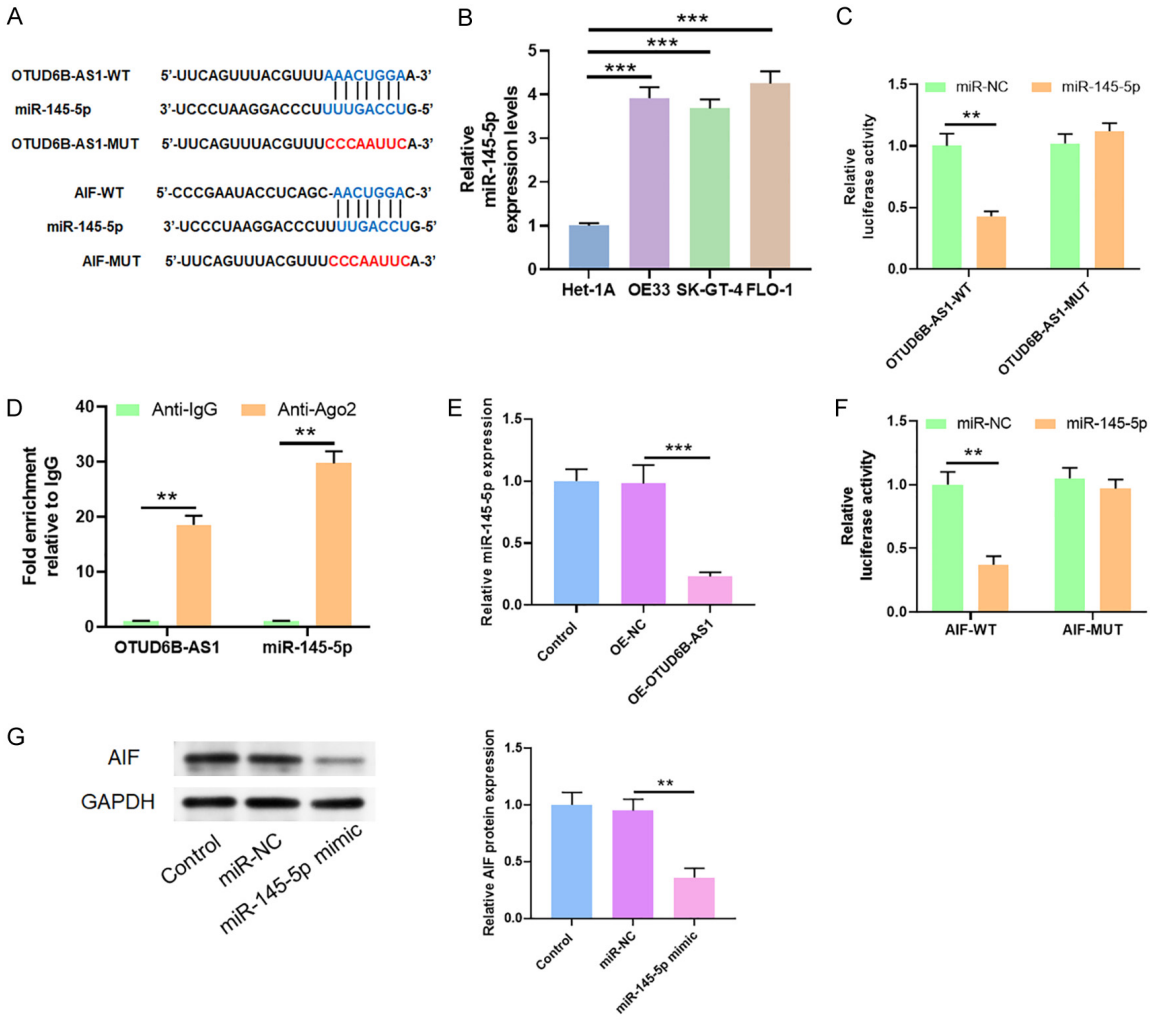

Figure 4. OTUD6B-AS1 regulates the miR-145-5p/AIF axis through a ceRNA mechanism in EAC cells. A. Predicted binding sites between miR-145-5p and OTUD6B-AS1 or AIF 3'UTR. B. qRT-PCR analysis of miR-145-5p expression in EAC cell lines and Het-1A cells. C. Dual-luciferase reporter assay confirming the interaction between OTUD6B-AS1 and miR-145-5p. D. RNA Immunoprecipitation assay using anti-Ago2 antibodies showing enrichment of OTUD6B-AS1 and miR-145-5p in the RNA-induced silencing complex. IgG served as the positive control. E. qRT-PCR analysis of miR-145-5p level after OTUD6B-AS1 overexpression in OE33 and FLO-1 cells. F. Dual-luciferase reporter assays validating the interaction between miR-145-5p and the 3'-UTR of AIF. G. Western blot analysis of AIF protein expression in cells transfected with miR-145-5p mimics or their corresponding controls. $^{**}P<0.01$, $^{***}P<0.001$.

and elevated γ-H2AX levels in the OTUD6B-AS1 overexpression group (**Figure 6H**), suggesting enhanced DNA damage and activation of parthanatos-associated signaling.

Collectively, these findings support that OTUD6B-AS1 suppresses EAC development through modulation of the miR-145-5p/AIF axis and activation of parthanatos-related cell death pathways.

Discussion

Esophageal adenocarcinoma (EAC) remains one of the most lethal gastrointestinal malignancies, primarily due to its asymptomatic early stages and inherent resistance to conventional chemoradiotherapy [19]. Consequently, ongoing exploration to identify novel therapeutic targets has increasingly focused on the non-coding transcriptome. In this study, OTUD6B-AS1 was identified as a previously underexplored tumor-suppressive lncRNA in EAC. Specifically, OTUD6B-AS1 was significantly downregulated in EAC cell lines and OTUD6B-AS1 overexpression notably suppressed aggressive tumor behaviors. Mechanistically OTUD6B-AS1 was found to promote parthanatos in EAC cells through modulation of the miR-145-5p/AIF axis through a ceRNA mechanism.

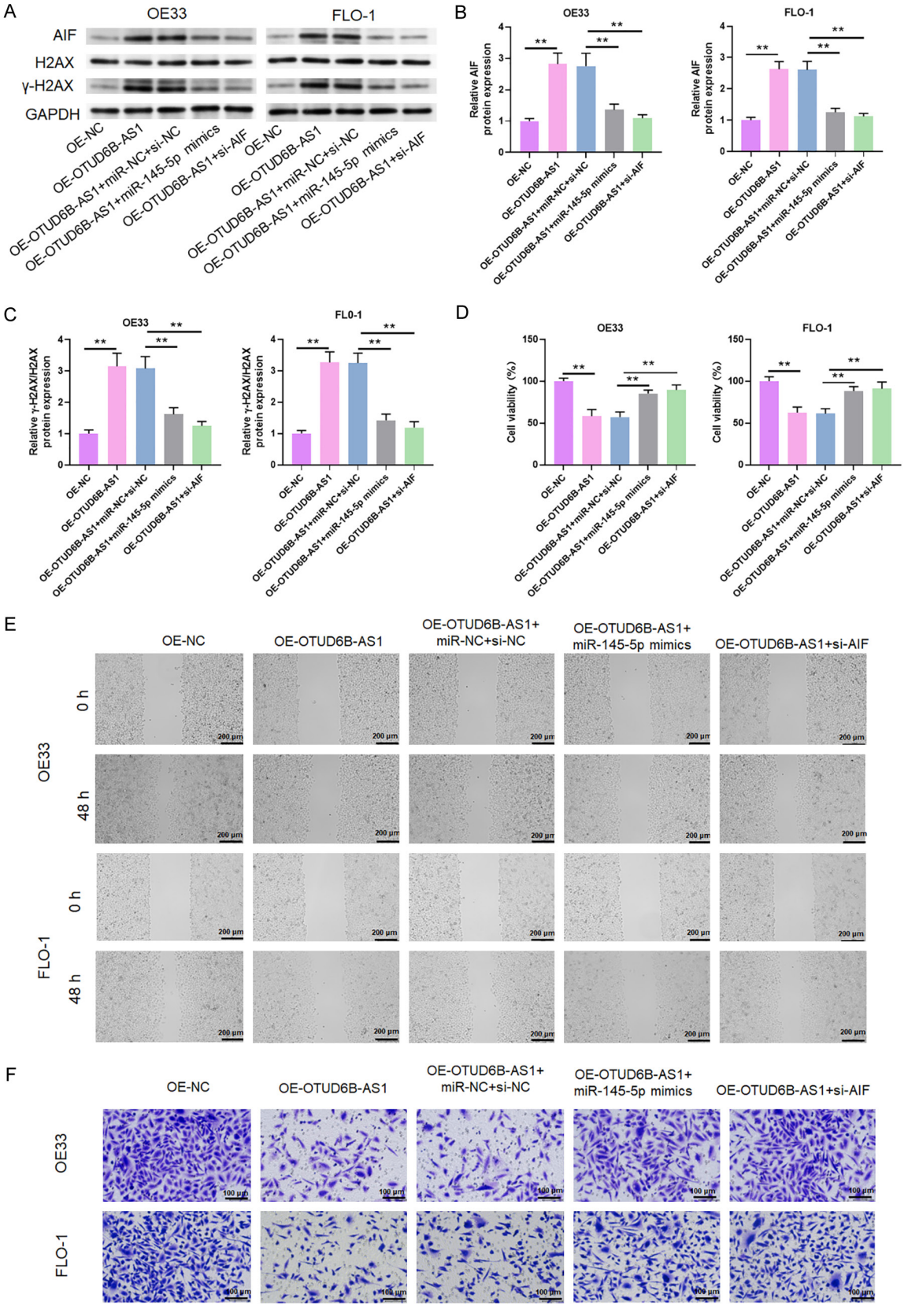
A
OE33
FLO-1
AIF
H2AX
γ-H2AX
GAPDH
OE-NC
OE-OTUD6B-AS1
OE-OTUD6B-AS1+miR-NC+si-NC
OE-OTUD6B-AS1+miR-145-5p mimics
OE-OTUD6B-AS1+si-AIF
B
Relative AIF protein expression
C
Relative γ-H2AX/H2AX protein expression
D
Cell viability (%)
E
0 h
48 h
200 μm
F
100 μm

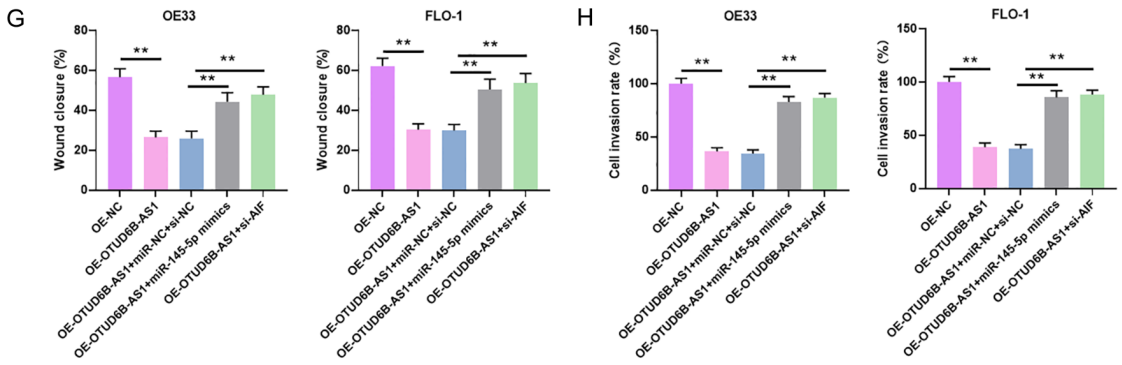

Figure 5. Functional rescue of the miR-145-5p/AIF axis in OTUD6B-AS1-mediated tumor suppression and parthanatos-associated phenotypes in EAC cells. (A-C) Western blot analysis of AIF and γ-H2AX expression in OTUD6B-AS1-overexpressing cells co-transfected with miR-145-5p mimic or si-AIF. (D) CCK-8 assay measuring cell viability in each rescue group. (E-H) Wound healing (E, G) and Transwell invasion (F, H) assays evaluating the reversal of OTUD6B-AS1-mediated inhibition of migration and invasion after miR-145-5p overexpression or AIF knockdown. Scale bar = 200 μm; Scale bar = 100 μm. $^{**}P<0.01$.

The subcellular localization of lncRNAs is context-dependent, and their intracellular distribution are critical for functional regulatory mechanisms [20]. Over the past decade, evidence supports that OTUD6B-AS1 exerts context-dependent and even opposing roles in different tumors. In breast cancer, it has been reported to act as an oncogene, whereas in clear-cell renal-cell carcinoma, it functions as a tumor suppressor [17, 21, 22]. In the present study, we further clarified its expression profile in esophageal tissues and found that OTUD6B-AS1 was markedly downregulated in EAC cells. Its predominant cytoplasmic localization provides an essential basis for miRNA sponging, consistent with the canonical ceRNA regulatory mode.

One of the key findings of our study is that restoration of OTUD6B-AS1 expression activates parthanatos-associated cell death. This process is characterized by PARP-1 activation and subsequent nuclear translocation of AIF. Mechanistically, OTUD6B-AS1 overexpression enhanced PARP-1 expression and promoted AIF nuclear accumulation, both of which are crucial for activating parthanatos. Additionally, OTUD6B-AS1 overexpression significantly increased the number of DNA double-strand breaks (γ-H2AX positive cells), and was associated with enhanced PARP-1 activity. Under physiologic conditions, AIF resides mainly in mitochondria, where it participates in oxidative phosphorylation. However, upon cellular stress, it translocates to the nucleus, where it contributes to chromatin condensation and cell death [5, 23]. Notably, EAC is frequently characterized by dysfunction of apoptotic signaling pathway, including p53 mutation and dysregulation of Bcl-2 proteins, which contribute to resistance to conventional apoptosis-inducing therapies [24, 25]. Therefore, induction of parthanatos may represent a feasible therapy to overcome apoptosis resistance. In this context, OTUD6B-AS1 may enhance the susceptibility of apoptosis-resistant malignant cells to programmed cell death by activating non-apoptotic death pathways.

Mechanistically, we further delineated the role of the OTUD6B-AS1/miR-145-5p/AIF regulatory axis in the execution of parthanatos. Although miR-145-5p is widely recognized as a tumor suppressor in multiple malignancies, its biological function is highly context-dependent [26, 27]. In certain cancers, including advanced colorectal cancer, miR-145-5p has been reported to exhibit oncogenic properties by promoting tumor invasion and metastasis [28]. In EAC, increased miR-145 expression has also been associated with enhanced invasion and anoikis resistance [29], and has been implicated in tumor immune evasion [13]. In our EAC models, miR-145-5p was significantly upregulated and inhibited AIF translation, thereby suppressing parthanatos and promoting tumor cell survival. By sponging miR-145-5p, OTUD6B-AS1 relieved the inhibitory effects of miR-145-5p on AIF, thus restoring AIF protein expression. Consistently, OTUD6B-AS1 overexpression significant-

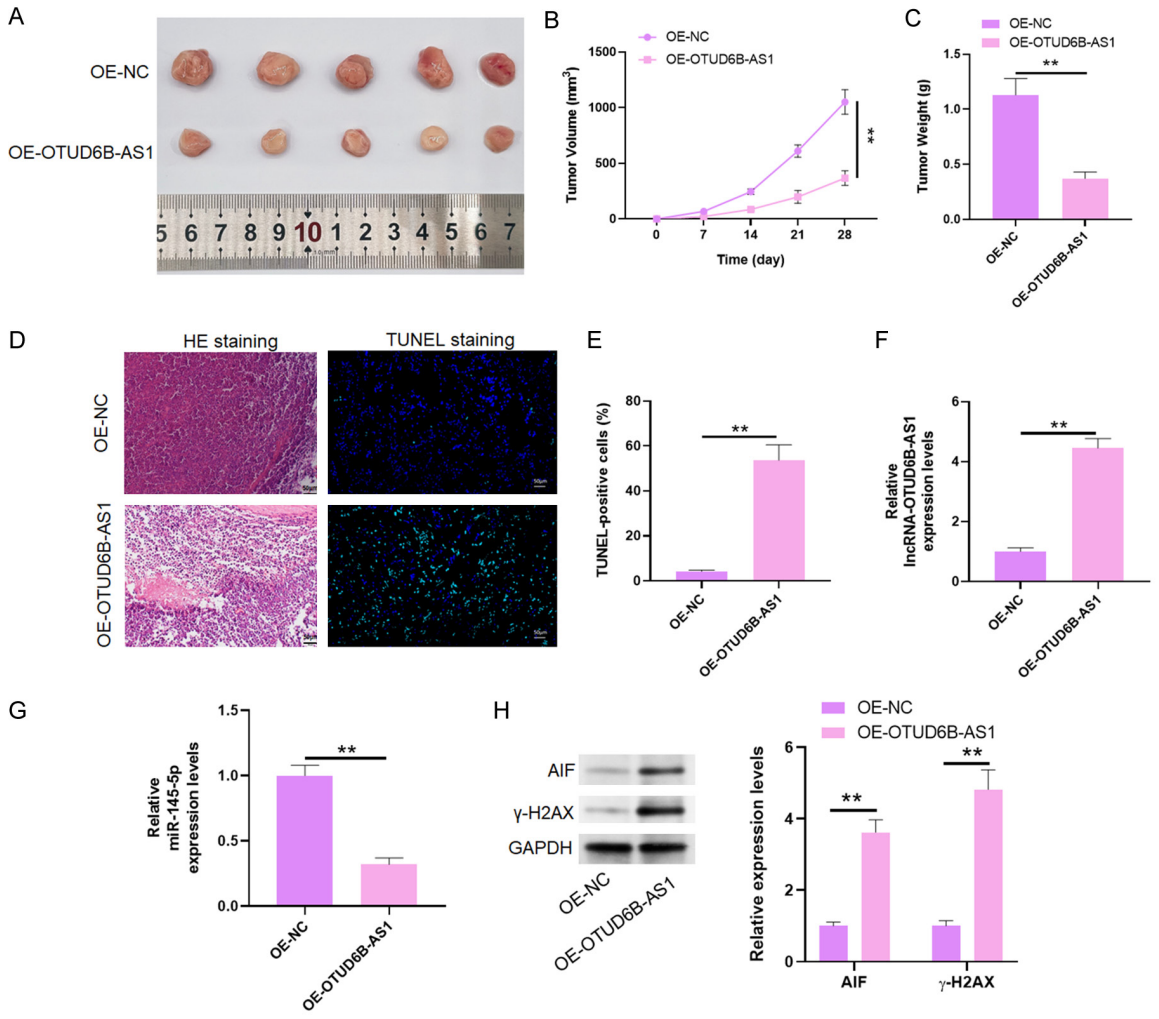

Figure 6. Effect of OTUD6B-AS1 on EAC tumor growth *in vivo* through the miR-145-5p/AIF axis. (A) Representative images of excised tumors from each group (n = 5/group). (B) Tumor growth curves over 28 days (n = 5/group). (C) Comparison of final tumor weight at the end of the experiment (n = 5/group). (D) Representative images of H&E staining and TUNEL staining of tumor tissues from different groups. Scale bar = 50 μm. (E) Quantification of apoptotic cells based on TUNEL staining in tumor sections. (F, G) qRT-PCR analysis of the OTUD6B-AS1 (F) and miR-145-5p (G) expression in xenograft tumor tissues (n = 5/group). (H) Western blot analysis of AIF and γ-H2AX protein expression in tumor tissue lysates (n = 5/group). $^{**}P<0.01$.

ly reduced xenograft tumor growth, accompanied by sustained miR-145-5p downregulation and activation of the AIF/γ-H2AX-associated cell death signature.

Due to several limitations inherent to pre-clinical studies, further investigation is required. First, our *in vivo* experiments were performed in immunocompromised mice, which do not fully recapitulate the complexity of the tumor immune microenvironment, thereby limiting the translational relevance of the findings. Second, although OTUD6B-AS1 overexpression was confirmed by qRT-PCR, potential off-target effects associated with supraphysiological lncRNA expression could not be excluded. Future studies using CRISPR activation (CRISPRa) systems or multiple independent knockdown/overexpression approaches would help address this limitation. Finally, although *in vivo* data showed tumor suppression accompanied by increased γ-H2AX accumulation and AIF expression, we did not directly confirm that parthanatos is the predominant model of cell death *in vivo*. Functional validation using co-staining of poly(ADP-ribose) polymers, nuclear AIF translocation, and cleaved caspase-3, as well as pharmacologic inhibition of PARP-1 or genetic knockdown

of AIF *in vivo*, would further strengthen mechanistic conclusions.

Conclusion

OTUD6B-AS1 suppresses EAC progression through a ceRNA network involving miR-145-5p, thereby relieving repression of AIF and promoting parthanatos-associated cell death. Clinically, the OTUD6B-AS1/miR-145-5p/AIF pathway may represent a target for overcoming apoptosis resistance in EAC.

Acknowledgements

This study was supported by the Quanzhou Municipal Science and Technology Plan Project (No. CQZ2024N0060289).

Disclosure of conflict of interest

None.

Address correspondence to: Xiangbo Chen, Gastrointestinal Endoscopy Room, Quanzhou First Hospital, No. 1028 Anji South Road, Fengze District, Quanzhou 362000, Fujian, China. E-mail: fjqzyycxb@163.com

References

[1] Yang H, Wang F, Hallemeier CL, Lerut T and Fu J. Oesophageal cancer. Lancet 2024; 404: 1991-2005.

[2] Baba Y, Tajima K and Yoshimura K. Intestinal and esophageal microbiota in esophageal cancer development and treatment. Gut Microbes 2025; 17: 2505118.

[3] Arbore G, Albarello L, Bucci G, Punta M, Cossu A, Fanti L, Maurizio A, Di Mauro F, Bilello V, Arrigoni G, Bonfiglio S, Biancolini D, Puccetti F, Elmore U, Vago L, Cascinu S, Tonon G, Rosati R, Casorati G and Dellabona P. Preexisting immunity drives the response to neoadjuvant chemotherapy in esophageal adenocarcinoma. Cancer Res 2023; 83: 2873-2888.

[4] Gaber CE, Sarker J, Abdelaziz AI, Okpara E, Lee TA, Klempner SJ and Nipp RD. Pathologic complete response in patients with esophageal cancer receiving neoadjuvant chemotherapy or chemoradiation: a systematic review and meta-analysis. Cancer Med 2024; 13: e7076.

[5] Gupta G, Afzal M, Moglad E, Goyal A, Almalki WH, Goyal K, Rana M, Ali H, Rekha A, Kazmi I, Alzarea SI and Singh SK. Parthanatos and apoptosis: unraveling their roles in cancer cell death and therapy resistance. EXCLI J 2025; 24: 351-380.

[6] Clune S, Awolade P, Esquer H, Zhou Q and La-Barbera DV. CHD1L in cancer and beyond: structure, oncogenic functions, and therapeutic potential. J Exp Clin Cancer Res 2025; 44: 167.

[7] Jiang X, Deng W, Tao S, Tang Z, Chen Y, Tian M, Wang T, Tao C, Li Y, Fang Y, Pu C, Gao J, Wang X, Qu W, Gai X, Ding Z, Fu Y, Zheng Y, Cao S, Zhou J, Huang M, Liu W, Xu J, Fan J and Shi Y. A RIPK3-independent role of MLKL in suppressing parthanatos promotes immune evasion in hepatocellular carcinoma. Cell Discov 2023; 9: 7.

[8] Zhang Y, Zhang C, Li J, Jiang M, Guo S, Yang G, Zhang L, Wang F, Yi S, Wang J, Fu Y and Zhang Y. Inhibition of AKT induces p53/SIRT6/PARP1-dependent parthanatos to suppress tumor growth. Cell Commun Signal 2022; 20: 93.

[9] Streppel MM, Pai S, Campbell NR, Hu C, Yabuuchi S, Canto MI, Wang JS, Montgomery EA and Maitra A. MicroRNA 223 is upregulated in the multistep progression of Barrett's esophagus and modulates sensitivity to chemotherapy by targeting PARP1. Clin Cancer Res 2013; 19: 4067-78.

[10] Robles-Remacho A, Zou Y, Grillo M and Nilsson M. Spatially resolved microRNA expression in tissues: technologies, challenges, and opportunities. Trends Genet 2025; 41: 1131-1143.

[11] Yu Y, Wang H, You C and Chen X. Plant microRNA maturation and function. Nat Rev Mol Cell Biol 2026; 27: 55-70.

[12] Ji Y, Wang L, Chang G, Yan J, Dai L, Ji Z, Liu J, He M, Xu H and Zhang L. Mir-421 and mir-550a-1 are potential prognostic markers in esophageal adenocarcinoma. Biol Direct 2023; 18: 5.

[13] Zhang L, Wang X, Li Y, Han J, Gao X, Li S and Wang F. c-Myb facilitates immune escape of esophageal adenocarcinoma cells through the miR-145-5p/SPOP/PD-L1 axis. Clin Transl Med 2021; 11: e464.

[14] Zhou W, Ji L, Liu X, Tu D, Shi N, Yangqu W, Chen S, Gao P, Zhu H and Ruan C. AIFM1, negatively regulated by miR-145-5p, aggravates hypoxia-induced cardiomyocyte injury. Biomed J 2022; 45: 870-882.

[15] Wang Q, Yan H, Zhang J, Zhang J, Su X and Su Z. Epigenetic modulation of cisplatin sensitivity by the M6A-linked ceRNA network in non-small cell lung cancer. Am J Physiol Cell Physiol 2025; 329: C481-C499.

[16] Su W, Guo C, Wang L, Wang Z, Yang X, Niu F, Tzou D, Yang X, Huang X, Wu J, Chen X, Zou L, Yang Z and Chen G. LncRNA MIR22HG abrogation inhibits proliferation and induces apoptosis in esophageal adenocarcinoma cells via

activation of the STAT3/c-Myc/FAK signaling. Aging (Albany NY) 2019; 11: 4587-4596.
[17] Wang G, Zhang ZJ, Jian WG, Liu PH, Xue W, Wang TD, Meng YY, Yuan C, Li HM, Yu YP, Liu ZX, Wu Q, Zhang DM and Zhang C. Novel long noncoding RNA OTUD6B-AS1 indicates poor prognosis and inhibits clear cell renal cell carcinoma proliferation via the Wnt/β-catenin signaling pathway. Mol Cancer 2019; 18: 15.
[18] Wang Z, Xia F, Feng T, Jiang B, Wang W and Li X. OTUD6B-AS1 inhibits viability, migration, and invasion of thyroid carcinoma by targeting miR-183-5p and miR-21. Front Endocrinol (Lausanne) 2020; 11: 136.
[19] Hoeppner J, Brunner T, Schmoor C, Bronsert P, Kulemann B, Claus R, Utzolino S, Izbicki JR, Gockel I, Gerdes B, Ghadimi M, Reichert B, Lock JF, Bruns C, Reitsamer E, Schmeding M, Benedix F, Keck T, Folprecht G, Thuss-Patience P, Neumann UP, Pascher A, Imhof D, Daum S, Strieder T, Krautz C, Zimmermann S, Werner J, Mahlberg R, Illerhaus G, Grimminger P and Lordick F. Perioperative chemotherapy or preoperative chemoradiotherapy in esophageal cancer. N Engl J Med 2025; 392: 323-335.
[20] Sharma S, Houfani AA and Foster LJ. Pivotal functions and impact of long con-coding RNAs on cellular processes and genome integrity. J Biomed Sci 2024; 31: 52.
[21] Li PP, Li RG, Huang YQ, Lu JP, Zhang WJ and Wang ZY. LncRNA OTUD6B-AS1 promotes paclitaxel resistance in triple negative breast cancer by regulation of miR-26a-5p/MTDH pathway-mediated autophagy and genomic instability. Aging (Albany NY) 2021; 13: 24171-24191.
[22] Zhang JN, Yi ZL, Zhou XR, Liu SS and Liu H. Dual role of lncRNA OTUD6B-AS1 in immune evasion and ferroptosis resistance: a prognostic and therapeutic biomarker in breast cancer. Noncoding RNA Res 2025; 14: 156-165.
[23] Zhou Y, Liu L, Tao S, Yao Y, Wang Y, Wei Q, Shao A and Deng Y. Parthanatos and its associated components: promising therapeutic targets for cancer. Pharmacol Res 2021; 163: 105299.
[24] Lian G, Malagola E, Wei C, Shi Q, Zhao J, Hata M, Kobayashi H, Ochiai Y, Zheng B, Zhi X, Wu F, Tu R, Nápoles OC, Su W, Li L, Jing C, Chen M, Zamechek L, Friedman R, Nowicki-Osuch K, Quante M, Que J and Wang TC. p53 mutation biases squamocolumnar junction progenitor cells towards dysplasia rather than metaplasia in Barrett's oesophagus. Gut 2025; 74: 182-196.
[25] Handa O, Goda K, Handa Y, Fukushima S, Osawa M, Murao T, Matsumoto H, Umegaki E, Fujita Y, Nishio K and Shiotani A. PDZK1 induces resistance to apoptosis in esophageal adenocarcinoma cells. Esophagus 2021; 18: 655-662.
[26] Chen X, Li D, Su Q, Ling X, Ding S, Xu R, Liu Z, Qin Y, Zhang J, Yang Z, Kang X, Qi Y and Wu H. MicroRNA-145-5p inhibits the tumorigenesis of breast cancer through SENP2-regulated ubiquitination of ERK2. Cell Mol Life Sci 2024; 81: 461.
[27] Wang L, Guo J, Lv C, Kong L, Cui J, Wang Z, Guo Y, Jia R, Guan T, Yu B and Li F. MiR-145-5p arrests the cell cycle by modulating SMAD5/cyclin D1 to inhibit gastric cancer progression. Front Cell Dev Biol 2025; 13: 1619359.
[28] Cheng X, Shen T, Liu P, Fang S, Yang Z, Li Y and Dong J. mir-145-5p is a suppressor of colorectal cancer at early stage, while promotes colorectal cancer metastasis at late stage through regulating AKT signaling evoked EMT-mediated anoikis. BMC Cancer 2022; 22: 1151.
[29] Derouet MF, Liu G and Darling GE. MiR-145 expression accelerates esophageal adenocarcinoma progression by enhancing cell invasion and anoikis resistance. PLoS One 2014; 9: e115589.